

The LAHET Code System with LAHET2.8

Richard E. Prael
Group X-5

David G. Madland
Group T-16

Los Alamos National Laboratory

LA-UR-00-2140
January 26, 2000

Contents

1	INTRODUCTION	1
1.1	About This Document	1
1.2	New Features in LAHET2.8	1
2	VARIANCE REDUCTION IN LAHET2.8	2
2.1	The IN and IMU Input Records	2
2.2	Impact of Cell Importances on the Contents of NEUTP	2
2.3	Impact of Cell Importances on Particle Decay Schemes	3
3	THE NUCLEON-NUCLEUS ELASTIC SCATTERING MODEL FOR LAHET	5
3.1	Introduction	5
3.2	LAHET Input Modification	5
3.3	Nucleon Elastic Scattering Cross Sections from 50 MeV to 400 MeV	6
3.4	Sampling Algorithm for the Angular Distribution	6
3.5	Effect of the Elastic Scattering	10
4	THE TRANSM CODE	13
5	USING MCNP VERSION 4B WITH LAHET	14
6	ADDITIONS AND CHANGES TO THE MANUAL	15
6.1	LAHET: Incoming Isotropic Source on a Sphere	15
6.2	LAHET: Change in Multiple Scattering Options	15
6.3	HTAPE: Isotopic Collision rates and CINDER Interface File	16
6.4	HTAPE: Cylinder Segmenting	16
6.5	HTAPE: Recoil Energy and Damage Energy Spectra	16
6.6	XSEX Tally Options	17

List of Figures

2.1	Sample importance listing.	3
2.2	Sample cell population table.	4
3.1	Elastic scattering cross sections for $A = 2, 4, 7, 9, 12$, and 16	7
3.2	Elastic scattering cross sections for $A = 27, 40, 56, 63, 81$, and 90	8
3.3	Elastic scattering cross sections for $A = 107, 138, 158, 184, 208$, and 238	9
3.4	Calculated center of mass angular distribution for 84 MeV neutrons scattered by ^{27}Al obtained from sampling algorithm.	10
3.5	Damage energy spectrum from 100 MeV protons incident on an 0.1 cm ^{27}Al target. . .	11
3.6	Damage energy spectrum from 100 MeV neutrons incident on an 0.5 cm ^{27}Al target. . .	11
3.7	256 MeV protons on Al^{27} . Longitudinal energy deposition.	12
3.8	256 MeV protons on Al^{27} . Proton angular distributions at 17.8 and 18.4 cm. depth. . .	12

Chapter 1

INTRODUCTION

1.1 About This Document

This document is intended as an interim publication to accompany the general release of the LAHET Code System (LCS) with LAHET2.8, to apply until a full manual revision may be completed. It is intended as a supplement to the original LCS manual[1] and the current MCNP manual[2]. It includes material previously released only as internal LANL documentation and as technical papers[3][4]. In addition, a summary of code features not included in the original manual, but distributed with the release of LAHET2.7, is included.

The user is expected to be familiar with the contents of the web site

<http://www-xdiv.lanl.gov/XCI/PROJECTS/LCS/>

and the many links available there. It is also recommended that the user subscribe to the e-mail group “lcs-forum”, which may be accomplished through the above site.

1.2 New Features in LAHET2.8

There are only two major features that distinguish LAHET2.8 from LAHET2.7. The first is the introduction of basic importance sampling in the style of MCNP for variance reduction in the particle transport process. The second is a more sophisticated description of elastic scattering for neutrons and now also for protons. Both are described in detail below.

In conjunction with the release of LAHET2.8, a new scheme for integrating MCNP into the LCS has been developed. In this method, low-energy neutrons from LAHET and photons from PHT are passed to MCNP Version 4B in the format of a “surface source read (SSR)” RSSA file. Surface crossing data from MCNP may be passed back to HTAPE for tallying in the format of an MCNP “surface source write (SSW)” WSSA file. A code TRANSM has been created to replace MRGNTP, combining the file merge feature of the latter with translation from NEUTP file format to RSSA file format. In addition, HTAPE has been modified to identify and read the input HISTX file in either the WSSA file format from MCNP or the original format used with the HMCNP series of codes.

With the release of MCNP Version 4B, all the features that required a separate HMCNP code are now included in the public release of MCNP. Thus HMCNP will no longer be supported and it is strongly suggested that the user employ MCNP Version 4B and its successors as part of the LCS.

Chapter 2

VARIANCE REDUCTION IN LAHET2.8

2.1 The IN and IMU Input Records

The IN input record, included in the MCNP-type records of a LAHET INH file, now represents true cell importances for the transport of nucleons, pions, and ions:

IN $I_1 I_2 \dots I_n$

where I_i is the importance for nucleons and pions in cell i and may take on any positive real value. A zero importance cell still represents an external void.

An additional input record has been introduced, also in MCNP input format, to permit the (optional) input of a different set of importances for muons; **it is not needed otherwise**. The IMU input record

IMU $J_1 J_2 \dots J_n$

provides for separate importances J_i for muons when executing a coupled nucleon-pion-muon problem (NBERTP = -1). The use of the IMU record applies only when $I_i \neq J_i$ in one or more cells; in the absence of an IMU record, $I_i = J_i$ for $i = 1, \dots, n$.

The output reflects the new input in the new listing of cell importances, as shown in figure 2.1. To assist the user in setting importances, a separate cell population table is produced for neutrons, all hadrons (neutrons, protons, pions, and ions), and muons as shown in figure 2.2.

2.2 Impact of Cell Importances on the Contents of NEUTP

The input parameter SWTM is used to initiate a roulette/splitting scheme for the particles recorded in NEUTP. For $SWTM \neq 0$, all particles written to NEUTP will have weight SWTM, determined by roulette or splitting with respect to the weight at which they appear; for $SWTM = 0$, no such game will be played.

Assigning real cell importances affects the use of SWTM in the following way. Let S_0 stand for the input parameter SWTM, and let S_i be the *effective* weight parameter used in cell i for the roulette/splitting scheme. Then

$$S_i = S_0/I_i$$

16 cells					
progr	probl			hadron	muon
name	name	mat	atom den	importance	importance
1	1	6666	0.00000E+00	1.00000E+00	1.00000E+00
2	2	1	-7.86000E+00	1.00000E+00	1.00000E+00
3	3	1	-7.86000E+00	1.00000E+00	1.00000E+00
4	4	1	-7.86000E+00	1.00000E+00	1.00000E+00
5	5	1	-7.86000E+00	1.00000E+00	1.00000E+00
6	6	1	-7.86000E+00	1.00000E+00	1.00000E+00
7	7	1	-7.86000E+00	1.00000E+00	1.00000E+00
8	8	1	-7.86000E+00	1.00000E+00	1.00000E+00
9	9	1	-7.86000E+00	1.00000E+00	1.00000E+00
10	10	1	-7.86000E+00	1.00000E+00	1.00000E+00
11	11	1	-7.86000E+00	1.00000E+00	1.00000E+00
12	12	1	-7.86000E+00	1.00000E+00	1.00000E+00
13	13	1	-7.86000E+00	1.00000E+00	1.00000E+00
14	14	6666	0.00000E+00	0.00000E+00	0.00000E+00
15	15	6666	0.00000E+00	0.00000E+00	0.00000E+00
16	16	6666	0.00000E+00	0.00000E+00	0.00000E+00

Figure 2.1: Sample importance listing.

so that the nominal weight of particles written to NEUTP is inversely proportional to the cell importance.

2.3 Impact of Cell Importances on Particle Decay Schemes

The input parameters WTPI ($\equiv W_\pi$) and WTMU ($\equiv W_\mu$) are used to provide weight control on decaying pions and emerging muons. The default values of WTPI and WTMU are still 0.1.

For coupled nucleon/pion/muon transport, muons are created with weight W_μ/J_i in cell i . Let W_0 be the pion weight before decay and let W be the pion weight after decay (which may be 0.) The pion weight after decay is constrained (by Russian roulette) to be either $W \geq W_{min}$, if possible, or $W = 0$, where $W_{min} = W_\pi/I_i$. For a muon, a similar constraint is applied with a minimum weight $W_{min} = W_\mu/J_i$. If the final weight is calculated to be $> W_{min}$, then it is further constrained by the condition that the decrement Δ in the pion or muon weight (weight to be decayed) be $\Delta \geq \Delta_{min}$ or $\Delta = 0$, where $\Delta_{min} = W_\mu/J_i$. The weight loss Δ is then obtained from the difference between the initial and final weight. In creating muons from pion decay, the mean number of muons emitted is $T_1 = \Delta J_i / W_\mu$ where Δ is the incremental weight loss of the pion through decay. The actual number emitted is given by $N = [T_1] + 1$ with probability $T_1 - [T_1]$ and $N = [T_1]$ otherwise.

If no muons are transported by the LAHET calculation, the above constraints are applied to determine the pion weight after decay. The pion weights before and after decay appear on the output HISTP file for input as the HISTIN file for a subsequent muon-only transport problem.

When muons are transported separately, using a HISTIN file produced by a LAHET execution in nucleon/pion only mode, the pion weight loss Δ is obtained from the pion data on HISTIN. Muons are then created with weight W_μ/J_i . The mean number of muons emitted is again $T_1 = \Delta J_i / W_\mu$,

population in cells:

progr	probl	neutron	hadron	muon
name	name	population	population	population
1	1	143.	1661.	0.
2	2	1243.	5438.	0.
3	3	1941.	5772.	0.
4	4	3315.	7988.	0.
5	5	2681.	5581.	0.
6	6	1847.	3391.	0.
7	7	1150.	1774.	0.
8	8	878.	1287.	0.

Figure 2.2: Sample cell population table.

with the actual number given by $N = [T1] + 1$ with probability $T1 - [T1]$ and $N = [T1]$ otherwise. No other constraints are applied to the allowed muon weight, and the importances J_i may differ from those used in the run which produced the HISTIN file.

Chapter 3

THE NUCLEON-NUCLEUS ELASTIC SCATTERING MODEL FOR LAHET

3.1 Introduction

LAHET[1] has been upgraded by the addition of an elastic scattering model for neutrons above 15 MeV and protons above 50 MeV. Earlier elastic scattering in LAHET had been limited to neutrons below 100 MeV using the Bechetti-Greenlees potential, input from the ELSTIN or LELSTIN data file. In the new approach, elastic scattering is allowed for neutrons above 20 MeV and protons above 50 MeV. The Monte Carlo methodology has been derived from the HERMES[5] code. However, the sampling algorithm for the center-of-mass scattering angle has been completely rewritten. More significantly, the elastic cross section data has been replaced below 400 MeV by using a global medium-energy nucleon-nucleus phenomenological optical-model potential[3]. This approach is an intermediate step in the effort to provide a library of both elastic and non-elastic cross sections from a global optical-model potential for LAHET usage.

3.2 LAHET Input Modification

The following input modifications relate to nucleon-nucleus elastic scattering.

- The input variable NELSTP (second on input record 5) is now called **IELAS** in the output and in documentation for this and later releases of LAHET.
- **IELAS = -1** : unchanged from previous definition for NELSTP = -1. Neutron elastic scattering is read from file ELSTIN and input variables NOELAS, NLEDIT, and ELAS are unchanged in meaning and use.
- **IELAS = 0** : no nucleon elastic scattering. NOELAS, NLEDIT, and ELAS are unused.
- **IELAS = +1** : new elastic scattering model for neutrons (only) at all energies (although the data range is 15 MeV to 22.5 GeV). NOELAS and ELAS are unused.

- **IELAS** = +2 : same as IELAS = +1; in addition, allows nuclear elastic scattering of protons above 50 MeV. This is the **DEFAULT**.
- For IELAS > 0, the default is NLEDIT = 1, thus printing the elastic cross section by energy and material; otherwise the default is NLEDIT = 0.

3.3 Nucleon Elastic Scattering Cross Sections from 50 MeV to 400 MeV

The tabulated elastic scattering cross sections were generated with an interim[3] global medium-energy nucleon-nucleus phenomenological optical-model potential. The potential is based upon a relativistic Schrödinger representation and is applicable to neutron and proton incident energies in the range 50 – 400 MeV and a target mass range of 20 – 220. The starting point for this work was the proton optical potential of Schwandt *et al.*[6] for the range 80 – 180 MeV.

This potential was modified to reproduce optimally experimental proton total reaction cross sections as a function of energy, while allowing only minimal deterioration in the fits to other elastic proton scattering observables. Further modifications in the absorptive potential were found necessary to extrapolate the modified potential to higher energies. At this point explicit isospin was introduced and the potential was converted to a neutron-nucleus potential by use of standard Lane model assumptions and by accounting approximately for the Coulomb correction. Final comparisons of predicted and measured elastic scattering observables for both protons and neutrons were made for ^{27}Al , ^{56}Fe , and ^{208}Pb [3]. The results were generally good.

The neutron and proton elastic cross sections so generated are tabulated in LAHET for 9 mass values and 20 energies between 50 MeV and 400 MeV. Above 400 MeV, the tabulations from HERMES are used, and the HERMES neutron elastic cross section tabulation below 50 MeV has been extended to lower and higher masses to minimize mass extrapolation error. Proton elastic scattering vanishes below 50 MeV in this implementation.

In figures 3.1, 3.2, and 3.3, the interpolated neutron and proton elastic cross sections to 10 GeV are shown for 18 mass values.

3.4 Sampling Algorithm for the Angular Distribution

The model[4] for the center of mass scattering angle is given by

$$\frac{d\sigma}{d\Omega} \sim \left(\frac{J_1(x)}{x} \right)^2 \text{ for } x = 2R \sin(\theta/2)/\bar{\lambda}, R = (1.4\text{fm})A^{1/3} + \bar{\lambda}$$

which, since $\cos \theta = 1 - \bar{\lambda}^2 x^2 / 2R^2$, provides a probability distribution for x^2 or $\cos \theta$. The implementation is by a table of 98 equally-probable (1%) bins in the variable x^2 , with an approximate asymptotic distribution for the last 2% of the distribution. In practice, the sampling range is always restricted by $\cos \theta \geq -1$.

In figure 3.4, a test calculation for $p(\cos \theta)$ vs. θ is shown for the center of mass angular distribution for 84 MeV neutrons scattered by ^{27}Al . The plot shown is an actual tabulation from sampling the distribution using 10^8 random samples of the algorithm. The locations of the first few zeros of the Bessel function in the distribution is apparent. The effect of using the equally-probable bins is also noticeable; each histogram step corresponds to 1% of the distribution.

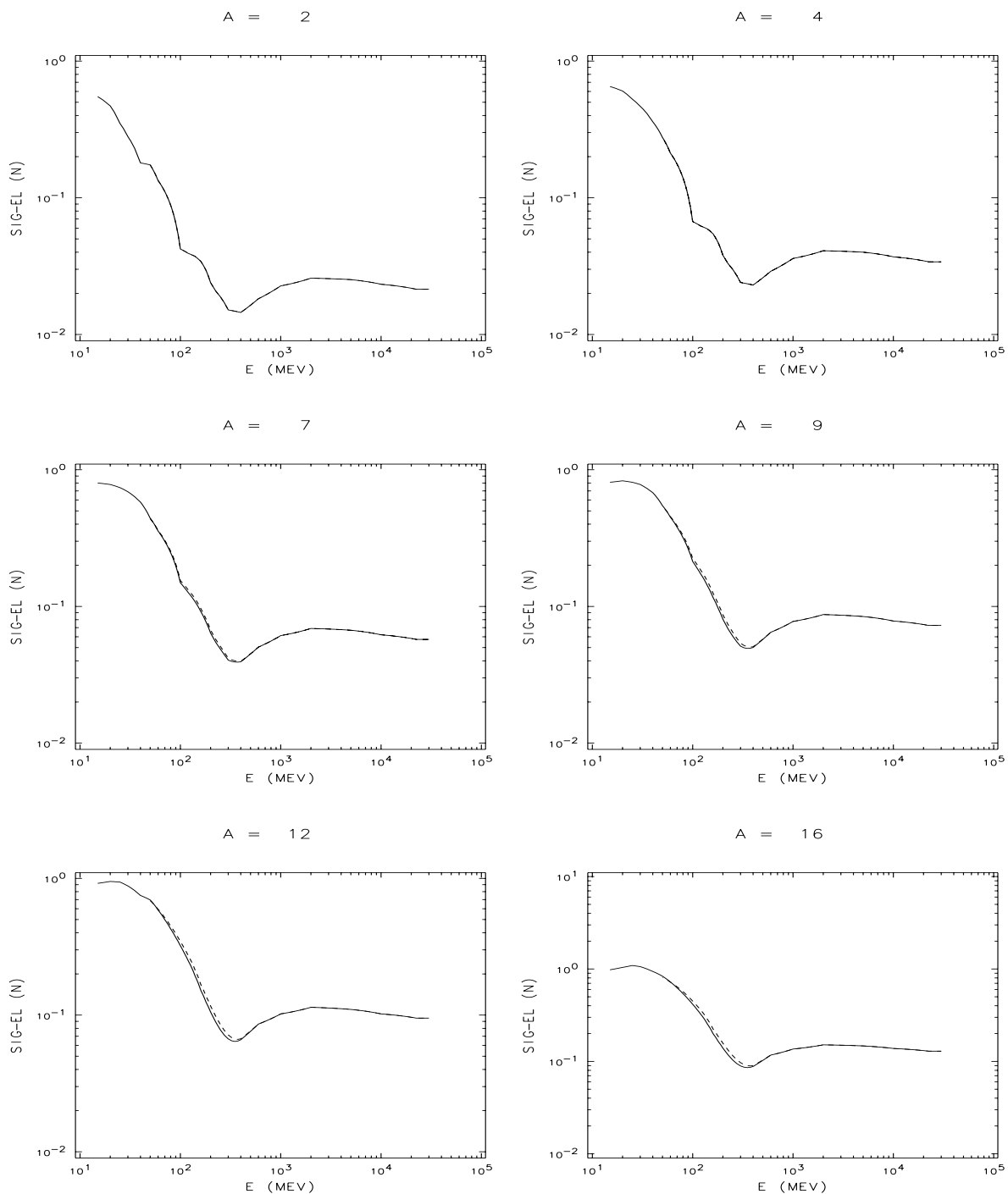


Figure 3.1: Elastic scattering cross sections for $A = 2, 4, 7, 9, 12$, and 16 . *Solid line* - neutrons; *dashed line* - protons.

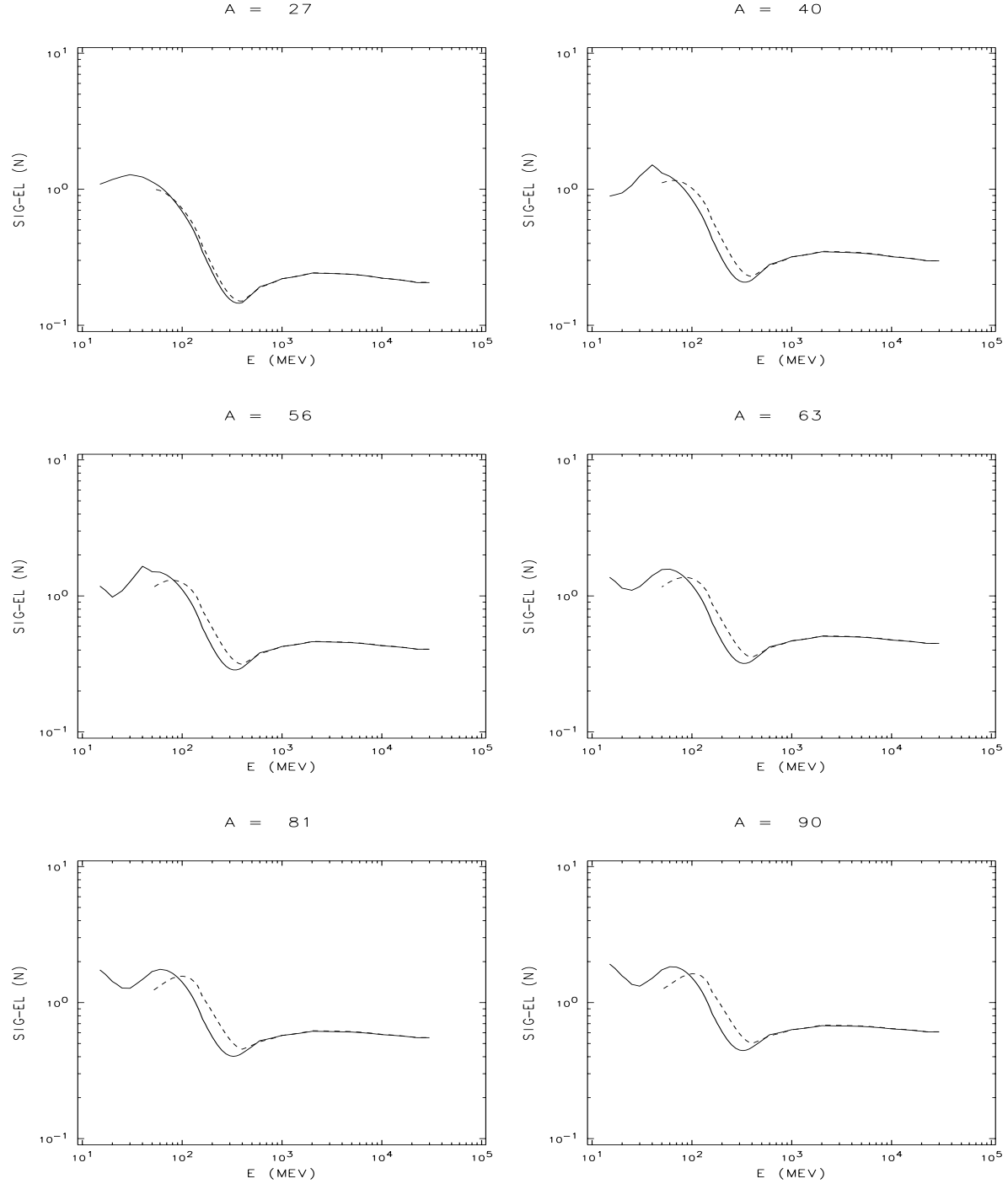


Figure 3.2: Elastic scattering cross sections for $A = 27, 40, 56, 63, 81,$ and 90 . *Solid line - neutrons; dashed line - protons.*

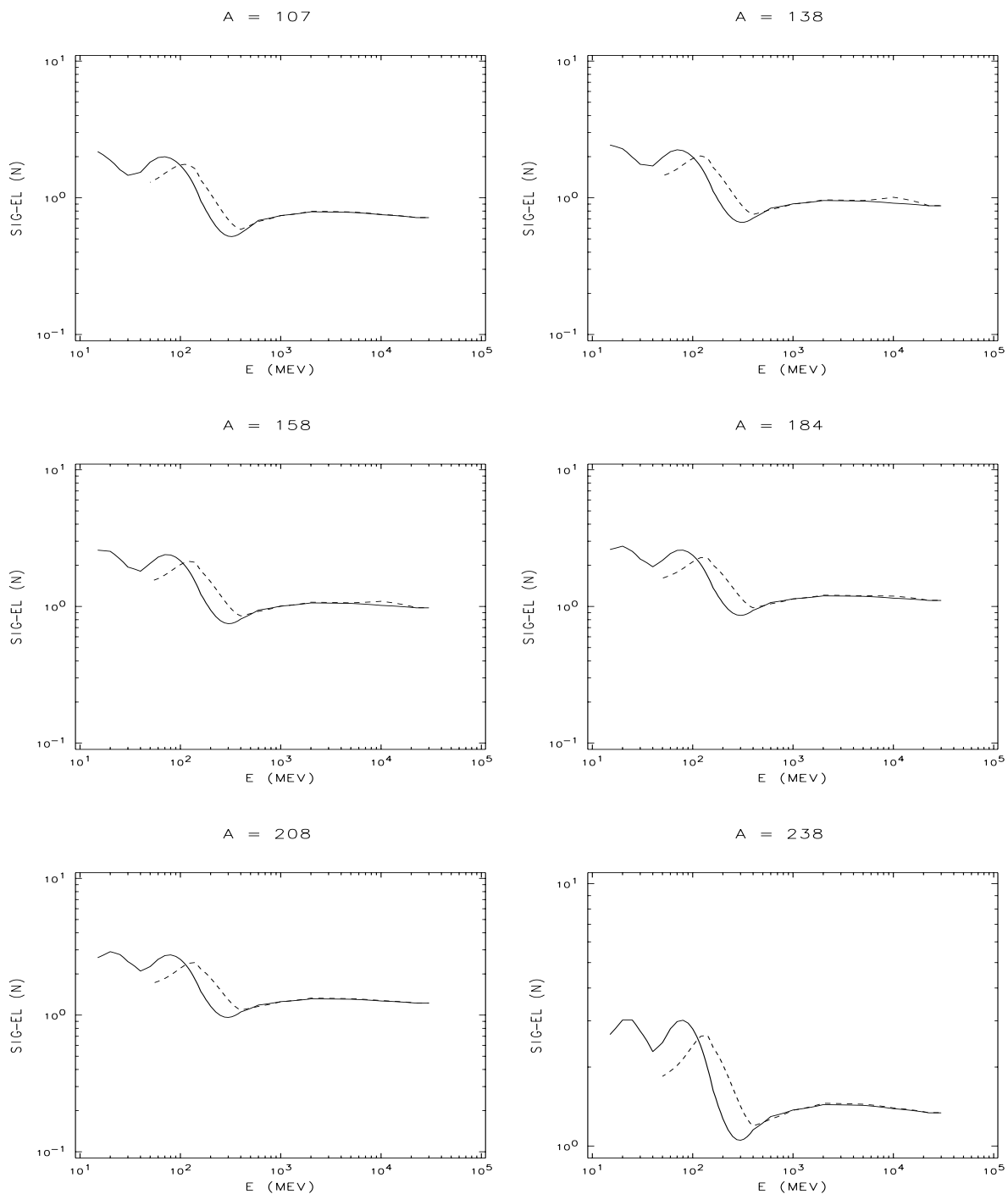


Figure 3.3: Elastic scattering cross sections for $A = 107, 138, 158, 184, 208$, and 238 . *Solid line - neutrons; dashed line - protons.*

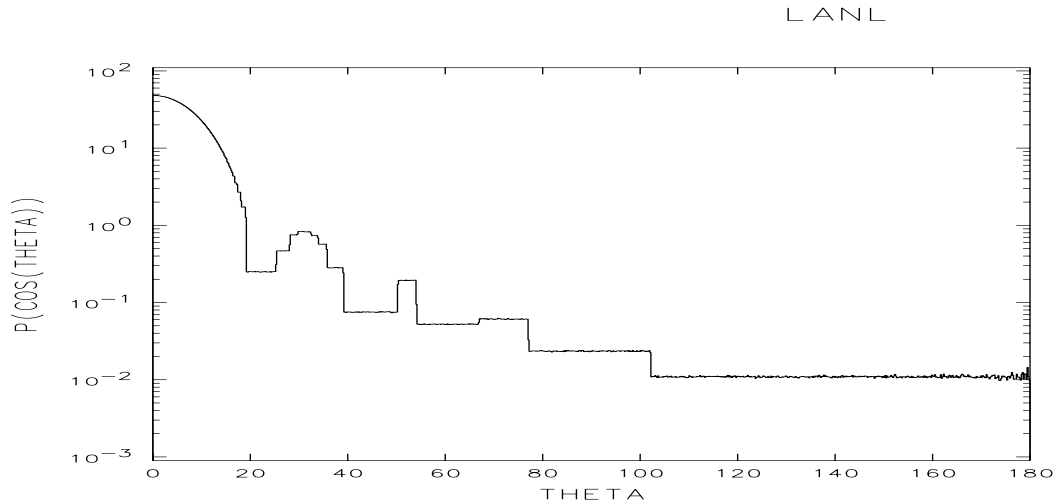


Figure 3.4: Calculated center of mass angular distribution for 84 MeV neutrons scattered by ^{27}Al obtained from sampling algorithm.

3.5 Effect of the Elastic Scattering

The presence of an elastic scattering channel in LAHET for protons (and neutrons above 100 MeV) adds entirely new calculational features. Most notably, damage calculations are modified by the effect of recoiling nuclei from proton elastic scattering above 50 MeV and from the improved neutron treatment at all energies. In our first example, figure 3.5, the damage energy spectrum is shown for 100 MeV protons on a 0.1 cm thick aluminum slab. The damage component from elastic scattering is a significant fraction of the total and would not have appeared in earlier LAHET calculations; in this example, the elastic contribution is 30% of the mean total recoil energy deposited and 41% percent of the mean total damage energy.

A second example of 100 MeV neutrons incident on 0.5 cm thick aluminum is shown in figure 3.6. The old treatment for neutron elastic scattering could adequately represent only the *mean* recoil energy deposition. The new method models the probability distribution of recoil energies in a more realistic manner and, as seen in figure 3.6, leads to an increase in the damage component; the change in the elastic treatment results in a 29% increase in the mean total recoil energy but a 69% increase in the mean total damage energy.

The presence of a proton elastic scattering channel provides another mechanism for energy deposition through recoil of the target nuclei. It also provides another mechanism for beam divergence. The magnitude of the effect can be seen in the next two figures, where the effects of proton elastic scattering are contrasted to multiple scattering of protons.

In figure 3.7, a longitudinal energy deposition calculation (MeV/cm) is shown. The elastic scattering deposits energy at higher energies and lowers the energy deposition peak without shifting it greatly. The two mechanisms produce effects, however, of comparable magnitude. Continuing the proton elastic scattering below 50 MeV might change the results by a small amount.

In figure 3.8, the dispersion of the proton beam is shown at two depths. (The line with *neither* elastic or multiple scattering corresponds to the background of secondary protons). Again we see that at this depth, near the end of the range, the angular effects from the two processes are of comparable magnitude. The Gaussian nature of the multiple scattering dispersion is very noticeable; the angular distribution from elastic scattering has a much longer tail.

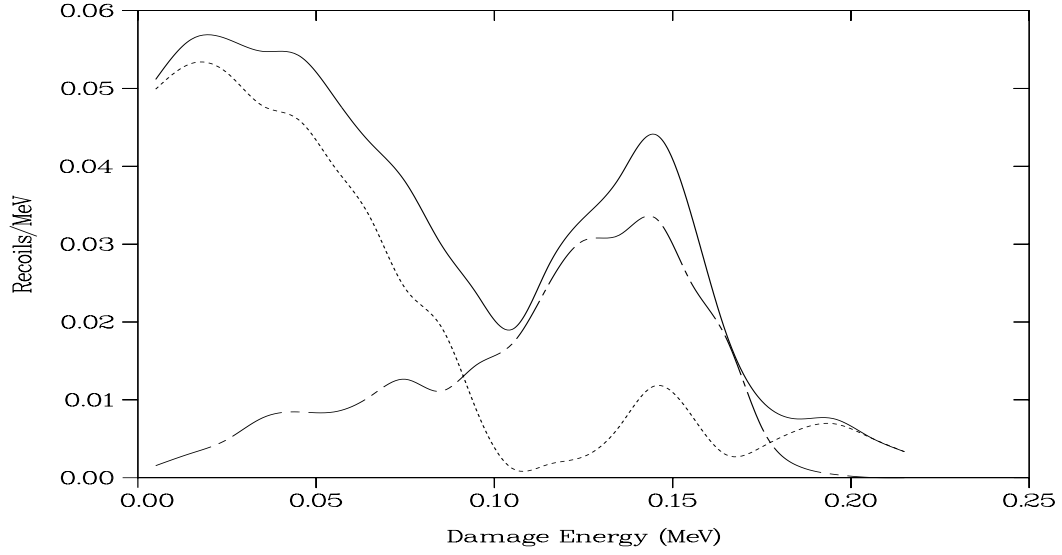


Figure 3.5: Damage energy spectrum from 100 MeV protons incident on an 0.1 cm ^{27}Al target. The *dashed* line represents the elastic contribution, the *broken* line the nonelastic, and the *solid* line the total. Previously, the total would have been identified with the broken line.

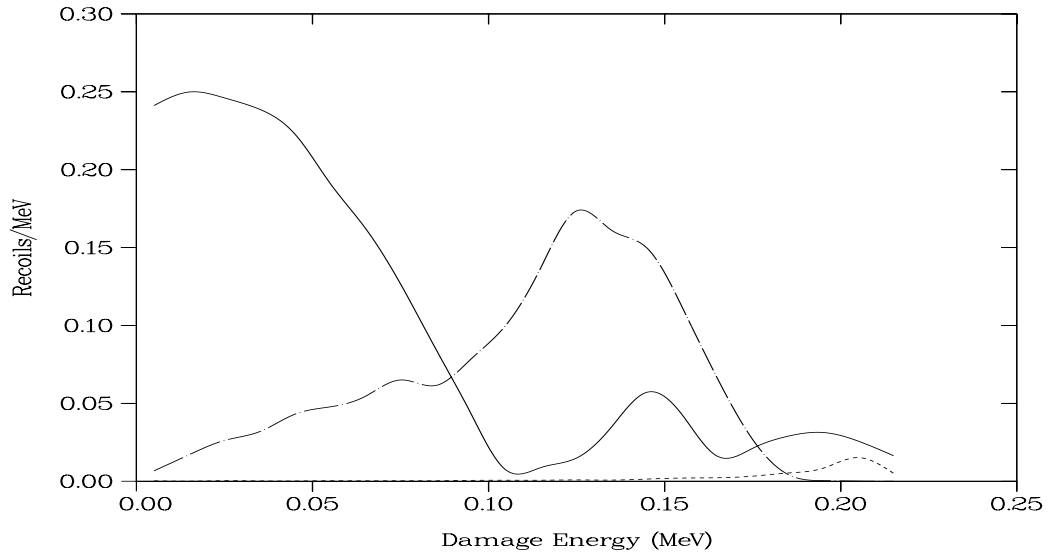
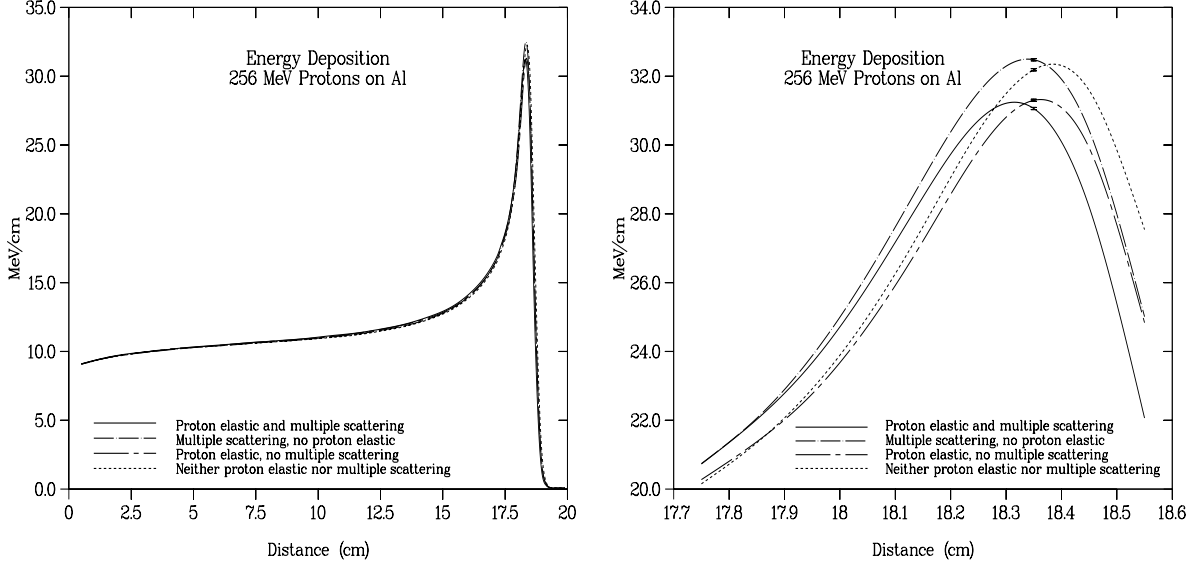
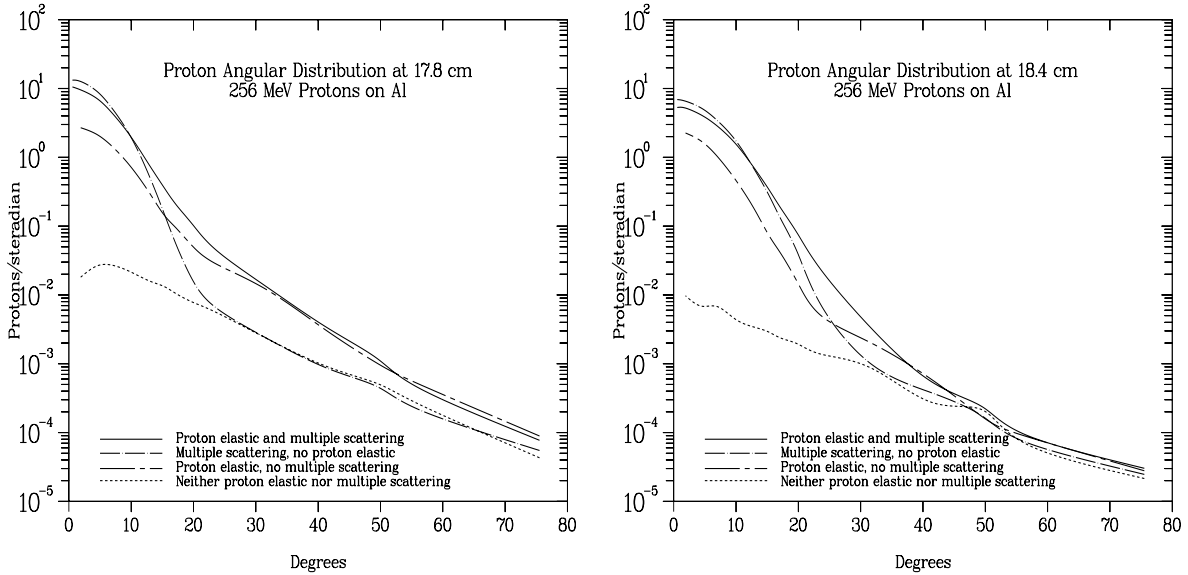


Figure 3.6: Damage energy spectrum from 100 MeV neutrons incident on an 0.5 cm ^{27}Al target. The *solid* line represents the *new* elastic contribution, the *dashed* line the *old* elastic contribution, and the *broken* line the nonelastic contribution (unchanged).

Figure 3.7: 256 MeV protons on Al^{27} . Longitudinal energy deposition.Figure 3.8: 256 MeV protons on Al^{27} . Proton angular distributions at 17.8 and 18.4 cm. depth.

Chapter 4

THE TRANSM CODE

The TRANSM code plays much the same role as the MRGNTP [2] with one exception. The output file is in the format of an MCNP “**surface source read (SSR)**” **RSSA file**, which may be input to any recent version of MCNP. As with MRGNTP, file specification information need be given only if the user is defining file names by file replacement. The input file names are the same as for MRGNTP; only the default output file name (RSSA) differs. The default file names are as follows:

NTP1	the first input file
NTP1A	the first continuation of the first file
NTP1B	the second continuation of the first file
NTP1C	the third continuation of the first file
NTP2	the second input file
NTP2A	the first continuation of the second file
NTP2B	the second continuation of the second file
NTP2C	the third continuation of the second file
RSSA	the output file.

The NEUTP files produced by LAHET do not use system familying routines in generating continuations. Consequently, the names may be changed at will to coincide with the MRGNTP/TRANSM default file names (although only three continuations are allowed). The GAMTP and GAMTP1 files produced by PHT have continuation files created by the system familying methods. For these, only the initial file is referenced by MRGNTP or TRANSM; the continuations are automatically accessed by the code. However, the continuation files in this case must be in the user’s local file space with the same name as that with which they were written.

Note: in problems with multiple usage of MRGNTP, as in sample problem 1ADD, only the *last* execution of MRGNTP is replaced with TRANSM. For those cases for which an RSSA file is desired for input into MCNP, but no merge is to be done, the following syntax will suffice:

TRANSM NTP1=filename NTP2=0 RSSA=filename

A typical example which combines neutron records from LAHET (NEUTP) with gamma records from PHT (GAMTP) would use the execution line

TRANSM NTP1=NEUTP NTP2=GAMTP RSSA=filename

Chapter 5

USING MCNP VERSION 4B WITH LAHET

MCNP Version 4B [2] contains both

- all the coding and features of HMCNP4A;
- the new MCNP option to produce a “surface source write” WSSA file to be edited by HTAPE using the SSW output option.

No new coding was required in MCNP to use the volume particle source RSSA file produced by TRANSM. With the new modification to the SSW option, MCNP contains all the features originally developed for HMCNP. To use old HMCNP input files with MCNP, remove the FILES and FU input records and use the SSR and SSW options as described below,

To use the new source input option, generate an RSSA-type file using TRANSM as described above. Use the SSR source option. **Do not** define units 77, 78, etc. on the FILES input record.

For the new output file option, use the SSW output option in the INP file with the following form:

SSW S₁ S₂ ... S_n SYM=2

Do not define unit 70 on the FILES input record. The option “SYM=2” is new; it causes a surface crossing record to be written for a particle crossing in **either** direction across specified surface S_i. One way to input the WSSA file produced into HTAPE is to use the following syntax:

HTAPE HISTX=WSSA

HTAPE will determine the format of the input file from the header record.

Chapter 6

ADDITIONS AND CHANGES TO THE MANUAL

6.1 LAHET: Incoming Isotropic Source on a Sphere

A unit source over the whole sphere of radius R corresponds to a source emission rate of $1/4\pi R^2$ particles per cm^2 , and produces a uniform flux of $1/\pi R^2$ in the interior; the current across any plane segment in the interior is $1/4\pi R^2$ particles per cm^2 in either direction across the surface, or or $1/2\pi R^2$ total current. A unit source over a hemisphere of radius R corresponds to a source emission rate of $1/2\pi R^2$ particles per cm^2 . However, the flux averaged over the whole volume is still $1/\pi R^2$ particles per cm^2 .

- Use ISOPT = 5.
- Center of the sphere is (X0,Y0,Z0); radius is A0.
- The SMU parameter is used for the following options:
 - SMU = 0 puts source over entire sphere;
 - SMU > 0 puts source only on +Z hemisphere;
 - SMU < 0 puts source omly on -Z hemisphere.
- Input parameters B0 and CUTS are unused

6.2 LAHET: Change in Multiple Scattering Options

Negative values are now allowed for NSPRED. The interpretation is as follows:

- NSPRED = 0 : no multiple scattering;
- NSPRED > 0 : multiple scattering for incident charged particles (only);
- NSPRED < 0 : multiple scattering for ALL charged particles (new).

The limits and meaning for $\text{NSPRED} > 0$ previously used now apply to its magnitude $\text{ABS}(\text{NSPRED})$. The *default* is still $\text{NSPRED} = +1$. It may be expected that in most problems applying the multiple scattering algorithm to all charged particles will increase running time for little benefit in computing most quantities.

6.3 HTAPE: Isotopic Collision rates and CINDER Interface File

$\text{IOPT} = 8$ has been modified to produce a CINDER production rate input file for $\text{IXOUT} > 0$. The default file name is OPT8A.

Option $\text{IOPT} = 15$ has been added to provide a collision rate edit by target isotope. The input has the same meaning as for $\text{IOPT} = 8$, with the following exceptions:

- $\text{KOPT} = 0$ or 1 tabulates all collisions;
- $\text{KOPT} = 2$ or 3 tabulates neutron elastic scattering only;
- $\text{KOPT} = 4$ or 5 tabulates nonelastic events only.

If KOPT is even, the edit is by cell number; if KOPT is odd, the edit is by material number. $\text{IOPT} = 15$ will produce a CINDER removal rate input file for $\text{IXOUT} > 0$. The default file name is OPT15A.

6.4 HTAPE: Cylinder Segmenting

- Segmenting with cylinders applies to the same options as segmenting with planes; i.e., $\text{IOPT} = 1, 2$, or 11 .
- Segmenting cylinders are CONCENTRIC with an axis, not just parallel.
- The input has the same format as segmenting by planes; however, IFSEG negative designates cylindrical segmenting.
- The values of the FSEG array are the radii of nested concentric cylinders and must be in increasing order.
- $\text{IFSEG} = -1$ indicates that the segmenting cylinders are concentric with the x-axis; $\text{IFSEG} = -2$ indicates that the segmenting cylinders are concentric with the y-axis; $\text{IFSEG} = -3$ indicates that the segmenting cylinders are concentric with the z-axis.

6.5 HTAPE: Recoil Energy and Damage Energy Spectra

- Option $\text{IOPT} = 16$ has been added to provide an edit of the spectra of total recoil energy, neutron elastic recoil energy, total damage energy, and neutron elastic damage energy. Also estimated are the mean weight of recoiling fragments per history, mean weight of recoil (or damage) energy per history, and the mean energy per fragment (the ratio of the previous two estimates).
- NERG specifies the number of energy bins for the spectra; a minus sign on NERG will have the tabulation normed per MeV (recommended to produce a true spectrum).

- Input variables NTIM, NTYP, NFPRM, IXOUT, IRS, IMERGE, ITCONV, and IRSP are unused.
- KOPT = 0 indicates tally by cell; IOPT = 1 indicates tally by material. NPARM is the number of cells (or materials) to be read in for the tally.
- The damage energy U is obtained from the recoil energy E using a parameterization of the Lindhard function L(E): $U=E*L(E)$.
- For multiatomic materials, L(E) is obtained by averaging the monatomic L(E) over the atom densities of the components (the averaging is exact for the Bertini INC model, only approximate for the ISABEL INC model.)
- If a minus sign flag is used with IOPT (IOPT = -16), the weights tallied for the spectra will be multiplied by corresponding recoil (or damage) energy.

6.6 XSEX Tally Options

The option control record has been modified to include two new input options and now has the form

NERG,NANG,FNORM,KPLOT,IMOM,IYIELD

where the new variables have the following interpretation:

- IMOM = 0 : cross sections are tabulated vs. energy (MeV) and differential cross sections are calculated per unit energy (per MeV);
- IMOM \neq 0: cross sections are tabulated vs. momentum (MeV/c) and differential cross sections are estimated per unit momentum (per MeV/c);
- IYIELD = 0 : cross sections are estimated;
- IYIELD \neq 0 : yields are calculated with respect to the estimated nonelastic cross section.

Bibliography

- [1] Richard E. Prael and Henry Lichtenstein, “User Guide to LCS: The LAHET Code System”, Los Alamos National Laboratory report LA-UR-89-3014 (September 1989).
- [2] Judith F. Briesmeister, editor, “MCNPTM - A General Monte Carlo N-Particle Transport Code”, Los Alamos National Laboratory report LA-12625-M (March 1997).
- [3] D. G. Madland, *Proceedings of a Specialist’s Meeting on Preequilibrium Reactions, Semmering, Austria, February 10–12, 1988*, Edited by B. Strohmaier (OECD, Paris, 1988), p. 103–116.
- [4] R. E. Prael and D. G. Madland, “A Nucleon-Nucleus Elastic Scattering Model for LAHET”, *Proceedings of the 1996 Topical Meeting on Radiation Protection and Shielding, N. Falmouth, MA, April, 1996*, p. 251.
- [5] P. Cloth *et al.*, *HERMES - A Monte Carlo Program System for Beam-Materials Interaction Studies*, Kernforschungsanlage Jülich GmbH, Jül-2203, May 1988.
- [6] P. Schwandt *et al.*, Phys. Rev. C **26**, 55 (1982).